MABS
2016, VOL. 8, NO. 7, 1417–1424
http://dx.doi.org/10.1080/19420862.2016.1207031

Taylor & Francis
Taylor & Francis Group

REPORT

OPEN ACCESS

The CD25-binding antibody Daclizumab High-Yield Process has a distinct glycosylation pattern and reduced antibody-dependent cell-mediated cytotoxicity in comparison to Zenapax®

Bishu Ganguly[a], Balaji Balasa[a], Lyubov Efros[a], Paul R. Hinton[b], Stephen Hartman[c], Archana Thakur[b], Joanna M. Xiong[b], Brian Schmidt[c], Randy R. Robinson[d], Thierry Sornasse[a], Vladimir Vexler[a], and James P. Sheridan[a]

[a]Department Translational Medicine, AbbVie Biotherapeutics, Redwood City, CA, USA; [b]Department Discovery Sciences, AbbVie Biotherapeutics, Redwood City, CA, USA; [c]Department Analytical Development & QC, AbbVie Biotherapeutics, Redwood City, CA, USA; [d]Department of Neuroscience Development, AbbVie Biotherapeutics, Redwood City, CA, USA

ABSTRACT

The CD25-binding antibody daclizumab high-yield process (DAC HYP) is an interleukin (IL)-2 signal modulating antibody that shares primary amino acid sequence and CD25 binding affinity with Zenapax®, a distinct form of daclizumab, which was approved for the prevention of acute organ rejection in patients receiving renal transplants as part of an immunosuppressive regimen that includes cyclosporine and corticosteroids. Comparison of the physicochemical properties of the two antibody forms revealed the glycosylation profile of DAC HYP differs from Zenapax in both glycan distribution and the types of oligosaccharides, most notably high-mannose, galactosylated and galactose-α-1,3-galactose (α-Gal) oligosaccharides, resulting in a DAC HYP antibody material that is structurally distinct from Zenapax. Although neither antibody elicited complement-dependent cytotoxicity in vitro, DAC HYP antibody had significantly reduced levels of antibody-dependent cell-mediated cytotoxicity (ADCC). The ADCC activity required natural killer (NK) cells, but not monocytes, suggesting the effects were mediated through binding to Fc-gamma RIII (CD16). Incubation of each antibody with peripheral blood mononuclear cells also caused the down-modulation of CD16 expression on NK cells and the CD16 down-modulation was greater for Zenapax in comparison to that observed for DAC HYP. The substantive glycosylation differences between the two antibody forms and corresponding greater Fc-mediated effector activities by Zenapax, including cell killing activity, manifest as a difference in the biological function and pharmacology between DAC HYP and Zenapax.

Abbreviations: ADCC, antibody-dependent cell-mediated cytotoxicity; AICC, antibody-independent cell-mediated cytotoxicity; Alpha-Gal, galactose-α-1,3-galactose; CDC, complement-dependent cytotoxicity; CPM, counts per minute; DAC HYP, daclizumab high-yield process; E:T, effector to target; FACS, fluorescence-activated cell sorting; GSH, glutathione; GST, glutathione S-transferase; IL, interleukin; MOA, mechanism of action; MS, multiple sclerosis; ND, not detectable; NK, natural killer; PBMC, peripheral blood mononuclear cells; PK, pharmacokinetics; Treg, regulatory CD4 T cell

ARTICLE HISTORY
Received 23 March 2016
Revised 10 June 2016
Accepted 23 June 2016

KEYWORDS
Antibody-dependent cell-mediated cytotoxicity; CD25; CD16; complement-dependent cytotoxicity; daclizumab; Fc-gamma RIII; IL-2; multiple sclerosis; Zenapax

Introduction

Daclizumab is a humanized monoclonal antibody of the human IgG1 isotype that binds specifically to CD25, the α subunit of the human high-affinity interleukin-2 (IL-2) receptor.[1,2] Different forms of daclizumab have been developed. Zenapax® was approved by the US. Food and Drug Administration in 1997 for the prophylaxis of acute organ rejection in patients receiving renal transplants, to be used in combination with an immunosuppressive regimen that included cyclosporine and corticosteroids, but later withdrawn from the marketplace for commercial reasons, not for safety reasons.[3] A second form, known as daclizumab high-yield process (DAC HYP), has completed pivotal clinical trials and received approval as a treatment for multiple sclerosis under the name ZinbrytaTM.[4,5] Both forms of daclizumab prevent IL-2 binding to CD25, thereby reducing IL-2 signaling by cells that require high-affinity IL-2 receptors to mediate IL-2 signaling, such as effector T cells implicated in the pathology of MS.[3,6] Multiple direct and indirect effects related to blocking IL-2 association with CD25 may be responsible for the immune modulatory activities of daclizumab, including direct inhibitory effects on secretion of inflammatory cytokines; expansion of regulatory CD56^{bright} natural killer (NK) cell activities; inhibition of the sustained expression of the T-cell expressed co-stimulatory molecule CD40L; and reductions in the priming

CONTACT James P. Sheridan james.sheridan@abbvie.com AbbVie Biotherapeutics Inc., Preclinical Sciences, 1500 Seaport Blvd., Redwood City, CA 94063, USA
Supplemental data for this article can be accessed on the publisher's website.

of antigen naïve T cells as a consequence of inhibiting trans-presentation of IL-2 by antigen-presenting cells.[7-11]

The direct killing of CD25-expressing effector T cells does not appear to be a significant contributing mechanism to the activity of DAC HYP as a treatment for MS.[2] Consistent with that hypothesis, the beneficial effects of treatment by DAC HYP appear within weeks of treatment initiation, whereas reductions in levels of effector T cells are modest and occur over months.[4] Because DAC HYP was developed as a subcutaneously administered long-term treatment for relapsing forms of MS, we sought to better understand the glycosylation profile of DAC HYP versus Zenapax antibodies and how glycosylation might relate to Fc-mediated cell killing activities for each antibody material.

Results

The DAC HYP glycosylation profile differs from Zenapax in both glycan distribution and the types of oligosaccharides formed

The glycan profile for DAC HYP is more homogeneous in comparison to Zenapax based on the distinguishing oligosaccharide peaks representing G0F-GlcNAc, G0F, G1F, Man5, Man6, Man7, G2F, and sialylated glycans (Fig. 1). Zenapax contains oligosaccharides not present in DAC HYP, including several high mannose forms (Man6, Man7) that are non-fucosylated (Table 1).

An additional glycosylation difference between DAC HYP and Zenapax is the presence of galactose-α-1,3-galactose (α-Gal) oligosaccharides. Antibodies produced in murine cell lines such as NS0 cells may contain α-Gal oligosaccharides when glycans are galactosylated. Alpha-Gal glycans were undetectable in DAC HYP (data not shown). The absence of α-Gal on DAC HYP is consistent with the very low level of galactosylation. However, α-Gal has been found to be present in Zenapax.[12]

Additionally, the heavy chain N-terminal sequence of DAC HYP was evaluated by cation exchange chromatography and was found to be distinct from Zenapax as a result of post-translational modification. Three distinct N-terminal heavy chain charge variants were observed: 1) heavy chain N-terminal glutamine, 2) heavy chain N-terminal pyroglutamate resulting from the post-translational conversion of N-terminal glutamine, and 3) heavy chain N-terminal glutamine fragment containing a remaining valine-histidine-serine (VHS) sequence

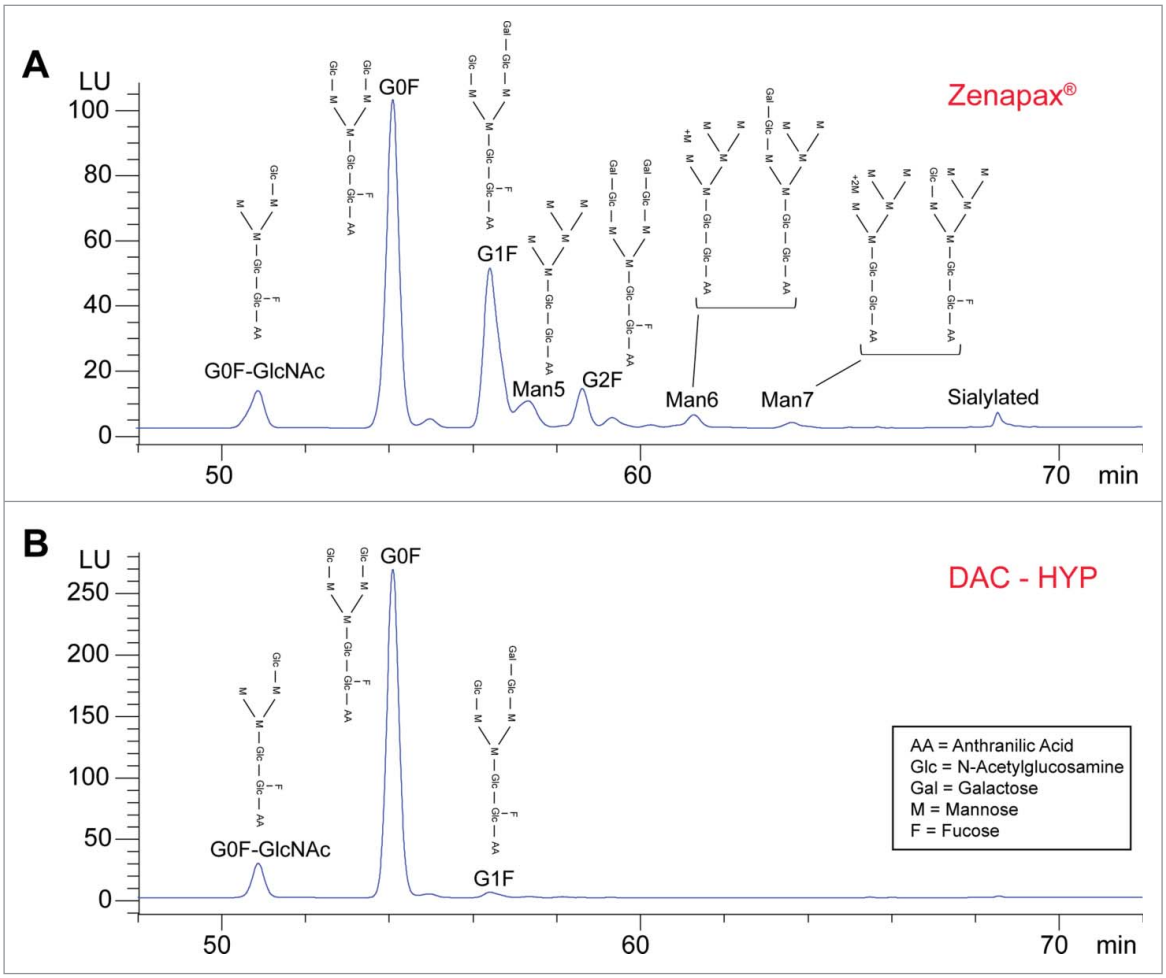

Figure 1. N-glycan profiles for Zenapax and DAC HYP. The relative abundance of N-linked glycans is shown for Zenapax (A) and DAC HYP (B) following enzymatic release and separation using HPLC. Note Man6 and Man7 oligosaccharides were presented as multiple structures because their low abundance made single homogenous species identification impossible.

Table 1. Zenapax and DAC HYP N-glycan distribution results. Approximately 95% of the N-linked glycans of DAC HYP are composed of G0F and G0F-GlcNAc forms, resulting in reduced heterogeneity in comparison to Zenapax. ND = not detectable.

Source	% G0F-GlcNAc	% G0F	% G1F	% G2F	% Man5	% Man6	% Man7	% Sialylated
Zenapax	6	46	27	5	6	5	1	2
DAC HYP	9	86	2	≤1	≤1	ND	ND	≤1

Table 2. Zenapax and DAC HYP interaction with CD25. Differences in glycosylation do not affect direct binding of Zenapax and DAC HYP to CD25 as determined by Biacore and inhibition of IL-2 dependent proliferation of KIT225/K6 cells in vitro.

	K_D (Biacore)	IC50 (IL-2 dependent proliferation)
Zenapax	3.2 nM	3.38 nM
DAC HYP	4.5 nM	3.14 nM

resulting from the incomplete cleavage of the signal sequence. Whereas DAC HYP contained 3 distinct heavy chain N-terminal isoforms, Zenapax only contained 2, lacking the native N-terminal glutamine isoform. (Fig. S1).

These differences in glycosylation and N-terminal processing of DAC HYP and Zenapax appear to have no effect on their direct interaction with CD25 because the relative potencies were very similar when analyzed for the binding affinity using surface plasmon resonance, and when analyzed for the ability to inhibit IL-2-dependent high-affinity IL-2 receptor-mediated cell proliferation in vitro (Table 2).

DAC HYP and Zenapax lack detectable complement-dependent cytotoxicity activity

Neither DAC HYP nor Zenapax elicited complement-dependent cytotoxicity (CDC) activity (assay schematic shown in Fig. S2), irrespective of whether assays were performed with pooled serum (Fig. 2A) or individual sera with low mannan (Fig. 2B) or high mannan binding lectin (Fig. 2C).

DAC HYP has significantly reduced antibody-dependent cell-mediated cytotoxicity activity in comparison to Zenapax

Incubation of increasing concentrations of DAC HYP, Zenapax and a positive control antibody with peripheral blood mononuclear cells (PBMC) and ^{51}Cr-labeled CD25-expressing KIT225/K6 cells, which were the effector and target cells, respectively (assay schematic shown in Fig. S2), resulted in dose-dependent, statistically significant increases in antibody-dependent cell-mediated cytotoxicity (ADCC) of the target cells in comparison to levels observed for a humanized, isotype control antibody (Fig. 3A). At the maximum antibody concentration, the levels of ADCC induced by Zenapax were statistically significantly ($p < 8.1\times10^{-4}$) greater in comparison to levels observed for DAC HYP. Similarly, incubation of a fixed antibody concentration (1 ug/mL) with increasing ratios of effector cells to target cells resulted in increasing levels of ADCC activity in the presence of DAC HYP, Zenapax and a positive control antibody (Fig. 3B). At maximum ratios of effector to target cells, the levels of ADCC induced by Zenapax was statistically significantly ($p < 9.3 \times 10^{-4}$) greater in comparison to levels observed for DAC HYP.

ADCC mediated by DAC HYP and Zenapax requires NK cells but not monocytes

To further characterize the mechanism responsible for ADCC activity by DAC HYP and Zenapax in vitro, functional assays were performed to evaluate the contribution of NK and monocyte cells to ADCC activities. Positive selection using magnetic beads bound to antigens specific for NK and monocyte cells, respectively, were used to remove each immune subset from human PBMC and to compare the effects of their selective removal on ADCC of KIT225/K6 target cells. Whereas DAC HYP and Zenapax continued to mediate ADCC of CD25-expressing target cells in the absence of monocytes (Fig. 4A), the removal of NK cells eliminated ADCC activity by both antibodies (Fig. 4B), suggesting their ADCC activities were mediated by antibody Fc domain interaction with CD16 expressed on NK cells. Because CD8 T cells are also capable of expressing CD16, the selective removal of CD8-positive cells was also evaluated, but no effects on either DAC HYP- or Zenapax-mediated ADCC were observed (data not shown).

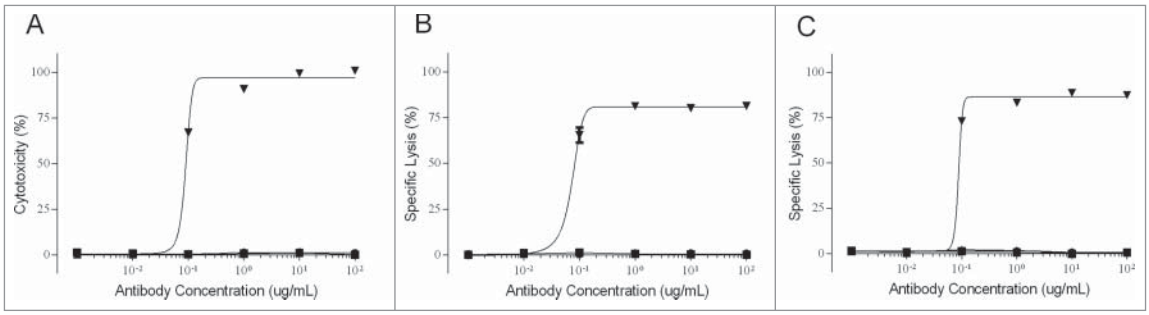

Figure 2. DAC HYP and Zenapax do not elicit CDC activity. Shown are mean and SE from 4 independent experiments evaluating DAC HYP (upward triangle), Zenapax (circle), a negative control antibody (square), and a CDC positive control antibody (downward triangle). CDC activity was undetectable for DAC HYP and Zenapax irrespective of whether the assay was performed using pooled serum (A), serum determined to have mannan lectin levels below 200 ng/mL (B) or greater than 3000 ng/mL (C).

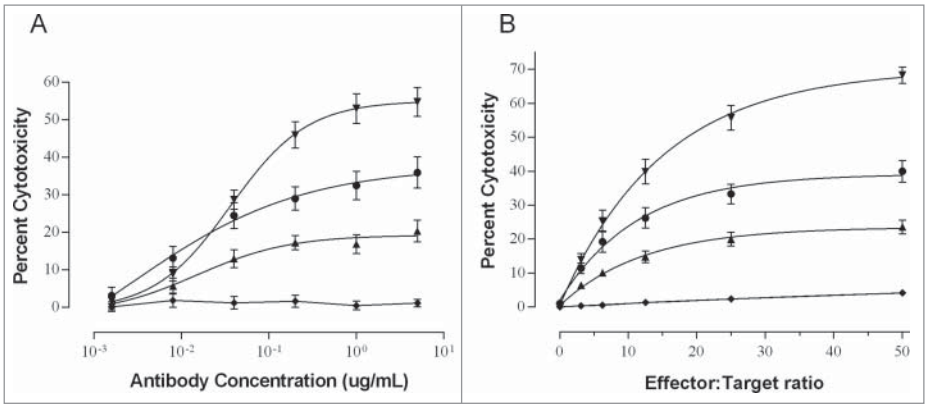

Figure 3. DAC HYP and Zenapax elicit ADCC activity in vitro. Mean and SE are shown for ADCC activities observed with increasing antibody concentrations (A), after AICC subtraction and normalization for specific lysis, evaluating DAC HYP (upward triangle), Zenapax (circle), a positive control antibody for ADCC (downward triangle), and isotype control antibody (diamond). Paired T test (2 tails) at maximum antibody concentration: DAC HYP versus IgG control ($p < 1.6\times10^{-3}$); Zenapax vs. DAC HYP ($p < 8.1\times10^{-4}$). ADCC activities were also evaluated using increasing ratios of effector to target cells (B) in the presence of fixed DAC HYP and Zenapax concentrations (1 ug/mL). Six independent experiments were performed for each assay. Curve fitting using log [agonist] versus response for a variable slope were calculated and are shown for DAC HYP, Zenapax and a positive control antibody for ADCC. Paired T test (2 tails) at maximum effector:target ratio: DAC HYP vs. IgG control ($p < 3.0 \times 10^{-5}$); Zenapax versus DAC HYP ($p < 9.3 \times 10^{-4}$).

DAC HYP has reduced binding interaction with a recombinant CD16 protein in vitro in comparison to Zenapax

Because antibody Fc interactions with CD16 are highly influenced by antibody Fc glycosylation, we developed an AlphaScreen™ bead proximity-dependent binding assay to examine whether differences could be detected in the binding interactions of DAC HYP and Zenapax for recombinant CD16 protein in vitro. Consistent with the reduced ADCC activity observed for DAC HYP in comparison to Zenapax, DAC HYP has significantly ($p < 0.02$, by Student's T test) reduced CD16 interaction in comparison to Zenapax at concentrations near the antibody EC_{50} concentration when evaluated using the AlphaScreen assay (Fig. 5).

Antibody Fc interaction with CD16 can result in activation and subsequent down-regulation of surface expressed CD16 levels.[13] We therefore sought to compare the differential effects of DAC HYP and Zenapax incubation on CD16 expression by NK cells when replicating the conditions of the in vitro ADCC assay. Incubation of PBMC for 4 hrs with Zenapax resulted in significantly ($p < 0.0157$) reduced CD16 surface expression levels on $CD3^-/CD56^+$ NK cells in comparison to effects observed for DAC HYP (Fig. 6). A potent ADCC inducing and CD16 interacting control antibody, clone Hu1D10, induced greater CD16 down-modulation (mean = 69%) in comparison to both Zenapax (mean = 36%) and DAC HYP (mean = 19%). Effects of IL-15 treatment (50 ng/mL), co-incubation with KIT255/K6 target cells, and incubation with isotype control antibody on CD16 down-modulation were not significant ($p > 0.05$). The decreased ability of DAC HYP to down-modulate CD16 expression on NK cells relative to effects observed for Zenapax correlated with the antibody's decreased interaction with CD16 and decreased ability to mediate ADCC in vitro.

Discussion

Structural glycosylation is a critical determinant of therapeutic antibody function, capable of affecting the biological function (i.e., bioactivity, immunogenicity and clearance rate from circulation) of therapeutic antibodies, based upon antibody Fc

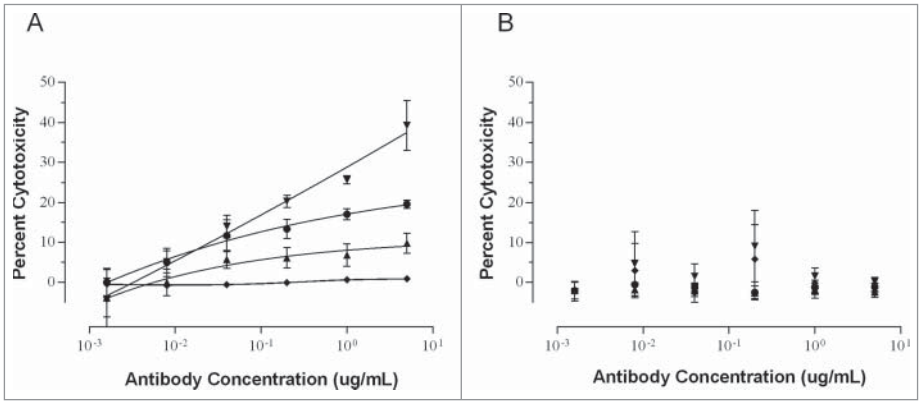

Figure 4. ADCC activity in the presence of increasing concentrations of DAC HYP and Zenapax following selective removal of monocyte and NK cells. Mean and SE are shown for ADCC activities observed with increasing antibody concentrations evaluating DAC HYP (upward triangle), Zenapax (circle), a positive control antibody for ADCC (downward triangle), and isotype control antibody (diamond). DAC HYP and Zenapax mediated ADCC of KIT225/K6 target cells in the absence of monocytes (A); however, the removal of NK cells eliminated ADCC activity by each antibody (B). Three independent experiments were performed for each assay. Curve fitting using log [agonist] vs. response for a variable slope were calculated and are shown for DAC HYP, Zenapax and a positive control antibody for ADCC in the presence of NK cells (A), but was not possible in the absence of NK cells (B).

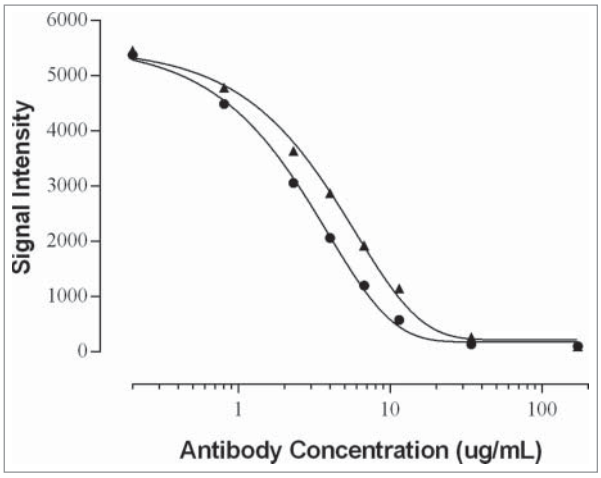

Figure 5. DAC HYP and Zenapax proximity interactions using a recombinant CD16 protein in vitro. Mean and SE signal intensities are shown for 3 independent evaluations using AlphaScreen when plotted against the competitor antibody concentration values for DAC HYP (upward triangle) and Zenapax (circle). Parallel line analysis reveals that Zenapax exhibits a mean potency for CD16 (V158) binding of 156% relative to the binding potency interaction observed by DAC HYP.

domain interactions with Fc receptors expressed on leukocyte cells.[14-16] Oligosaccharide mapping demonstrated that the glycan profile of DAC HYP is composed predominantly of 2 main N-glycans, G0F and G0F-GlcNAc, with much reduced glycoform heterogeneity compared to Zenapax. Notably, side-by-side comparative analysis of DAC HYP and Zenapax demonstrated significant differences in N-glycosylation. These structural differences between DAC HYP and Zenapax are attributable to distinct expression vectors, production cell lines and manufacturing processes. Although neither DAC HYP nor Zenapax exhibited detectable CDC, DAC HYP demonstrated significantly reduced ADCC activity in vitro compared to Zenapax. The maximal ADCC activity achieved with DAC

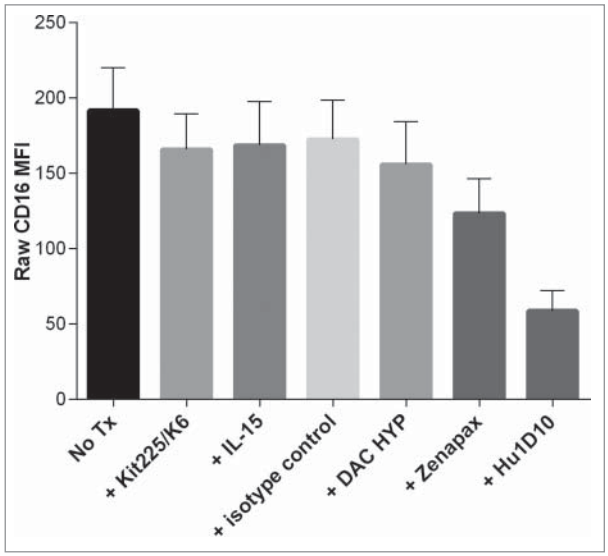

Figure 6. DAC HYP and Zenapax induce down-modulation of CD16 on NK cells. Incubation of PBMC with Hu1D10 antibody, Zenapax and DAC HYP caused significant ($p < 0.0157$) reductions in surface CD16 expression, as determined by flow cytometric staining of $CD3^-/CD56^+$ NK cells. Mean and SE results are shown for 7 independent experiments after normalizing mean fluorescence intensity (MFI) for CD16 to levels observed for no treatment.

HYP when evaluated as a dose response was ~30–40% lower than the activity elicited by the same concentration of Zenapax. The significant reduction in ADCC activity of DAC HYP is consistent with the observed differences in glycosylation profile, such as the reduction in high mannose non-fucosylated oligosaccharides that enhance ADCC activity in vitro and target cell depletion in vivo.[16] Levels of non-fucosylated high mannose glycans (sum of Man5, Man6, and Man7) in DAC HYP were very low (averages <1%) compared to levels for Zenapax (~10–12%).

Differences in ADCC activity likely result from decreased binding of DAC HYP to CD16, the NK cell-expressed Fc receptor that mediates this type of cell killing. Significant differences were observed for DAC HYP and Zenapax in terms of their binding interaction with recombinant CD16 protein in vitro. Additionally, the significant differences between DAC HYP and Zenapax binding to CD16 have effects on the activation status of NK cells, effects reflected in the decreased shedding of CD16 from NK cell surfaces of cells exposed to DAC HYP in comparison to Zenapax. These data establish that observed structural differences between DAC HYP and Zenapax lead to differences in biological activity. Because of these structural and biological activity differences, which could result in a product with a change in safety, purity, or potency, a complete manufacturing, preclinical toxicological and clinical assessment was performed for the purposes of understanding the unique activities of DAC HYP.[4,5,20]

High mannose glycans can also directly affect the pharmacokinetics (PK) of antibody therapeutics as a consequence of glycan-dependent Fc-receptor-mediated elimination, and may account for PK differences observed between DAC HYP and Zenapax.[17] In vivo studies in both humans and mice have shown that high mannose mAbs in general are cleared more rapidly from serum in comparison to other glycoform mAbs.[16,18,19] In comparison to Zenapax, the PK of DAC HYP has an apparent ~30% reduction in systemic clearance.[20] Therefore, the structural differences between DAC HYP and Zenapax are implicated in a change in human PK.

Although ADCC activity is directly linked to the mechanism of action (MOA) of some therapeutic antibodies, whether there is a link between ADCC activity and the MOA of DAC HYP as a treatment for MS is unclear. Multiple mechanisms related to IL-2 signaling modulation and the subsequent reductions in the T cell-mediated immune pathology have been hypothesized for both forms of daclizumab.[2,21] However, DAC HYP therapy of MS patients has also been observed to be associated with an ~50% reduction in circulating levels in an immune subset that expresses the highest levels of CD25, the FoxP3+ regulatory CD4 T cell (Treg) population.[22] Studies involving in vivo animal models have determined IL-2 signaling is required to maintain Treg homeostasis and cell numbers.[23-25] It is less clear whether DAC HYP's selective effects in blocking high affinity IL-2 receptor signaling are chiefly responsible for the reductions in Treg cell counts or whether ADCC-mediated cell killing contributes to some portion of these reductions. Regulatory T cell-mediated homeostasis with immune activated effector cells and the prevention of autoimmune pathologies are the result of a balance between these immune cell activities, and this balance is highly regulated by IL-2 signaling.[24-26] An increase in ADCC activity and a corresponding reduction in

Treg numbers has the potential to adversely affect that balance and adversely impact risk for autoimmune-related safety concerns. However, in aggregate the effect of DAC HYP on pro-inflammatory T cell-mediated activities and regulatory T cell counts has been associated with reductions in central nervous system autoimmune inflammation, while the risk of serious autoimmune disorders is very low.[4,5,27] In the context of the current understanding of the pathophysiology of MS, the lower ADCC activity of DAC HYP compared to Zenapax is hypothesized to be beneficial in terms of safety and potency by potentially limiting the reduction of CD25-expressing Tregs.

Materials and methods

Cell line generation and manufacture

Zenapax was manufactured by Hoffmann-La Roche, using the Celltech Biologics NS0 cell line transfected with the GS Gene Expression System™ (Lonza). DAC HYP was produced by AbbVie, using transfection of an NS0 sub-strain host cell line with a proprietary expression vector to create a new production cell line. The manufacturing process for DAC HYP utilizes a protein-free, animal component-free chemically defined medium, removing the risk of transmissible spongiform encephalopathy associated with animal derived components. The purification of DAC HYP uses a different process from Zenapax, including the use of a protein A affinity column separation, which captures and concentrates DAC HYP and removes host cell DNA, host cell protein, and other cell culture medium components.

Oligosaccharide mapping and N-terminal profiling

N-linked oligosaccharides present at the conserved Fc glycosylation site (Asn297) were enzymatically cleaved from the antibody backbone using the amidase PNGaseF. The enzymatically released oligosaccharides were subsequently derivatized with a fluorescent label and separated from the antibody via a nylon membrane. The labeled oligosaccharide mixture was then analyzed using normal phase high performance liquid chromatography (HPLC) with fluorescent detection. The chromatographic peaks resulting from the HPLC separation were assigned glycan identities based on comparison of their retention time to previously characterized glycan standards. The relative abundance of each glycan was calculated as a percentage of the total glycan peak area.

Characterization of N-terminal heavy chain variants was conducted using Cation Exchange Chromatography (CEX). Samples were enzymatically digested with papain and the resulting Fab and Fc fragments were chromatographically separated based on surface charge using a weak cation exchange column.

Plasmon resonance binding characterization using surface plasmon resonance

Antibody binding properties were characterized to determine rate constants (k_a and k_d) and affinity constant (K_D) for the binding interaction against soluble, recombinant human IL-2Rα (CD25) using Biacore technology. Each antibody material was immobilized on the chip surface using primary amine covalent coupling chemistry. Recombinant CD25 (R&D Systems, Cat. No. 223-2ACF) was injected at various concentrations in duplicate and reference surface for 2 minutes using an automated method. The binding data was corrected using a reference flow cell and buffer blank. The assay was replicated using a newly prepared sensor surface, and the binding data was then fit with BIAevaluation software (Biacore) using a bivalent model to obtain the equilibrium constants for kinetic evaluation.

Cell culture and isolation of effector cells

Relative antibody biological potencies for direct inhibition of IL-2-dependent high-affinity IL-2 receptor-mediated proliferation were determined using a cell-based method that evaluated effects of titrated antibody concentrations on the proliferation of the human leukemia cell line KIT225/K6.[28] PBMCs were isolated with Ficoll-Paque™ Plus density gradients (GE Healthcare Life Sciences) and used as the effector cells in ADCC assays. In additional ADCC experiments, monocyte and NK cells were removed from PBMC cultures using EasySep™ Human CD34 Positive Selection Kits (Stem Cell Technologies) for CD14 and CD56, respectively, and using the manufacturer's protocol for the Robosep™ Automated Cell Separation System (Stem Cell Technologies). Target cell depletion was found to be greater than 95% by flow cytometric analysis. All blood was obtained from informed consented healthy volunteers and no genotyping of individual donors was performed.

^{51}Cr-labeling of target cells

KIT225/K6 cells were grown in RPMI 1640 complete medium (10% heat inactivated fetal bovine serum plus supplements). KIT225/K6 cells were suspended in 0.5 mL of Assay Medium (RPMI 1640, 10% heat inactivated fetal bovine serum plus supplements) at a final concentration of 2×10^7 cells/mL, and labeled with 500 μCi of ^{51}Cr (50 μCi/10^6 cells) by incubating at 37°C in a water bath for 1 hr with occasional mixing. Labeled cells were washed 4 times with 12 mL of Assay Medium. The efficiency of target labeling was evaluated using the Beckman Gamma 5500B counter and considered acceptable if there was an activity of at least 20,000 cpm/10^5 cells. Labeled target cells were suspended at a cell density of 2.5×10^5 cells/mL in Assay Medium, or 5.0×10^5 cells/mL in CDC Assay Medium, as appropriate.

Complement-dependent cytotoxicity assay

Antibodies were diluted serially in CDC Assay Medium containing RPMI 1640, 0.1% BSA and 10 mM HEPES. 50 μL of ^{51}Cr-labeled target cells (25,000 cells/well) was added to the wells of a microtiter U-bottom 96-well plate, and then a volume of 50 μl of serial dilutions of test antibodies was added. 25 μl of 8% Triton X-100 and 25 μl of CDC Assay Medium were added to maximum-release wells and 50 μl of CDC Assay Medium was added to spontaneous release wells (quadruplicate). 50 μl of 1/3 dilution of human pooled serum was added to the reference and test sample wells. 50 μl of 1/3 dilution of heat inactivated (30 min at 56°C) human pooled serum was added to a complement-independent control, maximum release, and spontaneous release wells. The optimal human pooled serum concentration was pre-established by identifying the concentration at which the specific activity was maximal while the

non-specific activity was minimal. Assay plates were incubated for 2 hr at 37°C in a 7.5% CO_2 incubator and then spun at 350 RCF for 5 minutes at room temperature. A volume of 75 μl of supernatant was transferred to mini-tubes, and each mini-tube was inserted into a scintillation vial and counted for 1 minute in a Beckman Gamma 5500B counter, or equivalent. Pooled human serum was obtained from Quidel Corporation (San Diego, CA) or healthy volunteers using venipuncture and standard techniques.

The positive control antibody for CDC activity was the humanized IgG1/κ antibody, Hu#4, that has binding specificity for pan HLA-DR. The negative control antibody for both CDC and ADCC activity was the humanized IgG1/κ antibody HuFd79 that has binding specificity for an HSV viral antigen. Values reported as Percent Specific Lysis were derived using the following formula: Percent Specific Lysis = ((Antibody treatment counts per minute (CPM) – Spontaneous CPM) / (Maximum CPM – Spontaneous CPM)) × 100.

Antibody-dependent cell-mediated cytotoxicity assay

^{51}Cr-labeled KIT225/K6 cells (12,500 cells/well) were pre-incubated with a fixed concentration of 1 μg/mL mAb (for the variable effector to target [E:T] ratio format) or various doses (5, 1, 0.2, 0.04, 0.008, and 0.0016 μg/mL) of mAbs (for the variable antibody concentration format) for 30 minutes at 4°C in V-bottom 96-well plates in a volume of 100 μL of Assay Medium. Control cells were incubated with Assay Medium alone (no mAb) for subsequent determination of the spontaneous and maximum ^{51}Cr release, as well as antibody-independent cell-mediated cytotoxicity (AICC). PBMC (effectors) were diluted serially in Assay Medium, in a separate 96-well polypropylene plate, yielding concentrations of 6.25×10^5 cells/100 μL, 3.13×10^5 cells/100 μL, 1.56×10^5 cells/100 μL, 7.81×10^4 cells/100 μL, 3.91×10^4 cells/100 μL. 100 μL per well of PBMC suspension was transferred to the variable E:T ratio assay plate containing ^{51}Cr-labeled KIT225/K6 + 1 ug/mL mAbs, yielding E:T ratios of 50:1, 25:1, 12.5:1, 6.25:1 and 3.13:1. To the variable antibody concentration assay plate, PBMCs were diluted to 3.13×10^6 cells/100 uL and 100 uL per well was added to assay wells. 100 μL per well of Assay Medium alone (no effector) was added to ^{51}Cr-labeled KIT225/K6 + mAbs, to determine spontaneous and maximum release of ^{51}Cr. The assay plates were spun at 50 RCF for 2 minutes and incubated at 37°C in a 7.5% CO_2 incubator for 4 hrs. Thirty minutes before the end of the 4-hr incubation, a volume of 25 uL of 8% TritonX-100 was added to the appropriate control wells to determine the maximum release of ^{51}Cr from target cells. The positive control antibody for ADCC activity was the humanized IgG1/κ antibody Hu1D10 that has binding specificity for the HLA-DR β chain.

AlphaScreen™ assay for CD16 binding

DAC HYP and Zenapax antibody Fc binding to Fc-gamma RIII (CD16) were analyzed using a competitive bead-based proximity assay based on Perkin Elmer's AlphaScreen™ technology and an FcγRIIIa-V158 (CD16) GST (glutathione-S-transferase) fusion protein (gift from Biogen). GSH (glutathione) donor beads (Perkin Elmer) were used in combination with AlphaScreen-Acceptor beads (Perkin Elmer) conjugated to daclizumab materials. Triplicate dilution series of DAC HYP and Zenapax were added to GST-CD16 (V158) in 96-well plates. A mixture of AlphaScreen GSH-donor beads and daclizumab-acceptor beads was added to all the wells in assay buffer (1 × PBS with 0.1% BSA and 0.01% Tween 20, pH 7.2). Plates were incubated 4 hrs at room temperature in the dark and then read using an EnVision™ (Perkin Elmer) plate reader. The dose-dependent loss of fluorescent signal was used to quantify displacement of the reference DAC-acceptor bead conjugate from GSH donor beads coupled to GST-CD16. Parallel line analysis of the raw data was performed using PLA 1.2 to determine the potency for competitive inhibition of the bead proximity-based AlphaScreen signal. Paired, nonparametric Wilcoxon tests were performed using non-normalized measurements of MFI. Relative potency values were determined by calculating the distance between the parallel regression lines according to the formula:

$$\text{Log2 (Relative Potency)} = \left(\text{Yintercept}_{\text{sample}} - \text{Yintercept}_{\text{standard}}\right)/\text{slope}.$$

FACS determination of CD16 expression on NK cells

Fluorescence-activated cell sorting (FACS)-based measurements of Zenapax and DAC HYP binding effects on CD16 expression of NK cells were performed on PBMC derived NK cells cultured similar to the conditions used in the in vitro ADCC assays. Purified NK cells were isolated from PBMC using positive selection antibody cocktail with Robsep as described above and added at a final ratio of 25:1 effector to target NK cells. Various antibody treatments (5 ug/mL) and control NK activating cytokine IL-15 (50 ng/mL) were added in the presence of KIT225/K6 plus NK cells and incubated 4 hrs in a humidified CO_2incubator before staining with fluorescently labeled antibodies for FACS. FACS was performed using BD Biosciences solutions, equipment and antibodies specific for NK cells (CD56, Cat. No. 340723) and CD16 (Cat. No. 338426).

Inhibition of IL-2-dependent proliferation

Relative potencies of Zenapax and DAC HYP were determined using the human KIT225/K6 cell line that requires IL-2 for proliferation. Antibody was titrated against a unit volume of cells in the presence of IL-2 in a microtiter tissue culture plate and reduction of Alamar blue was determined using 530 nm excitation and 590 nm emission wavelengths. Potencies were determined by plotting the relative fluorescence units against the log10 of concentration values to produce sigmoidal curves and evaluated using a 4-parameter fit in SoftMax Pro 4.3 software.

Disclosure of potential conflicts of interest

All authors were employed by AbbVie Biotherapeutics or its predecessors, receiving stock and/or stock options, at the time the study was conducted. Currently, B. Ganguly is employed by Rinat/Pfizer, P.R. Hinton is employed by IGM Biosciences, T. Sornasse is employed by Genentech Inc., and V. Vexler is employed by Coherus Biosciences. In the last year, L. Efros was employed by BD Biosciences and J.M. Xiong worked at Rinat/Pfizer.

Funding

This study was funded by AbbVie Biotherapeutics which participated in the study design, research, data collection, analysis and interpretation of data, writing, reviewing, and approving the manuscript for publication.

References

1. Waldmann TA. Anti-Tac (daclizumab, Zenapax) in the treatment of leukemia, autoimmune diseases, and in the prevention of allograft rejection: a 25-year personal odyssey. J Clin Immunol 2007; 27:1-18; PMID:17216565; http://dx.doi.org/10.1007/s10875-006-9060-0
2. Bielekova B. Daclizumab therapy for multiple sclerosis. Neurotherapeutics 2013; 10:55-67; PMID:23055048; http://dx.doi.org/10.1007/s13311-012-0147-4
3. Vincenti F, Kirkman R, Light S, Bumgardner G, Pescovitz M, Halloran P, Neylan J, Wilkinson A, Ekberg H, Gaston R, et al. Interleukin-2-receptor blockade with daclizumab to prevent acute rejection in renal transplantation. Daclizumab Triple Therapy Study Group. N Engl J Med 1998; 338:161-65; PMID:9428817; http://dx.doi.org/10.1056/NEJM199801153380304
4. Gold R, Giovannoni G, Selmaj K, Havrdova E, Montalban X, Radue EW, Stefoski D, Robinson R, Riester K, Rana J, et al. Daclizumab high-yield process in relapsing-remitting multiple sclerosis (SELECT): a randomised, double-blind, placebo-controlled trial. Lancet 2013; 381:2167-75; PMID:23562009; http://dx.doi.org/10.1016/S0140-6736(12)62190-4
5. Kappos L, Wiendl H, Selmaj K, Arnold DL, Havrdova E, Boyko A, Kaufman M, Rose J, Greenberg S, Sweetser M, et al. Daclizumab HYP vs. interferon β-1a in relapsing multiple sclerosis. N Engl J Med 2015; 373:1418-28; PMID:26444729; http://dx.doi.org/10.1056/NEJMoa1501481
6. Sheridan JP, Robinson RR, Rose JW. Daclizumab, an IL-2 modulating antibody for treatment of multiple sclerosis. Expert Rev Clin Pharmacol 2014; 7:9-19; PMID:24308792; http://dx.doi.org/10.1586/17512433.2014.865516
7. McDyer JF, Li Z, John S, Yu X, Wu CY, Ragheb JA. IL-2 receptor blockade inhibits late, but not early, IFN-gamma and CD40 ligand expression in human T cells: disruption of both IL-12-dependent and -independent pathways of IFN-gamma production. J Immunol 2002; 169:2736-46; PMID:12193748; http://dx.doi.org/10.4049/jimmunol.169.5.2736
8. Bielekova B, Catalfamo M, Reichert-Scrivner S, Packer A, Cerna M, Waldmann TA, McFarland H, Henkart PA, Martin R. Regulatory CD56(bright) natural killer cells mediate immunomodulatory effects of IL-2Ralpha-targeted therapy (daclizumab) in multiple sclerosis. Proc Natl Acad Sci USA 2006; 103:5941-46; PMID:16585503; http://dx.doi.org/10.1073/pnas.0601335103
9. Snyder JT, Shen J, Azmi H, Hou J, Fowler DH, Ragheb JA. Direct inhibition of CD40L expression can contribute to the clinical efficacy of daclizumab independently of its effects on cell division and Th1/Th2 cytokine production. Blood 2007; 109:5399-406; PMID:17344465; http://dx.doi.org/10.1182/blood-2006-12-062943
10. Perry JS, Han S, Xu Q, Herman ML, Kennedy LB, Bielekova B. Inhibition of LTi cell development by CD25 blockade is associated with decreased intrathecal inflammation in multiple sclerosis. Sci Transl Med 2012; 4:1-8; PMID: 22855463; http://dx.doi.org/10.1126/scitranslmed.3004140
11. Wuest SC, Edwan JH, Martin JF, Han S, Perry JS, Cartagena CM, Matsuura E, Maric D, Waldmann TA, Bielekova B. A role for interleukin-2 trans-presentation in dendritic cell-mediated T cell activation in humans, as revealed by daclizumab therapy. Nat Med 2011; 17:604-09; PMID:21532597; http://dx.doi.org/10.1038/nm.2365
12. Stadlmann J, Pabst M, Kolarich D, Kunert R, Altmann F. Analysis of immunoglobulin glycosylation by LC-ESIMS of glycopeptides and oligosaccharides. Proteomics 2008; 8:2858-71; PMID:18655055; http://dx.doi.org/10.1002/pmic.200700968
13. Bowles JA, Wang SY, Link BK, Allan B, Beuerlein G, Campbell MA, Marquis D, Ondek B, Wooldridge JE, Smith BJ, et al. Anti-CD20 monoclonal antibody with enhanced affinity for CD16 activates NK cells at lower concentrations and more effectively than rituximab. Blood 2006; 108:2648-54; PMID:16825493; http://dx.doi.org/10.1182/blood-2006-04-020057
14. Arnold JN, Wormald MR, Sim RB, Rudd PM, Dwek RA. The impact of glycosylation on the biological function and structure of human immunoglobulins. Annu Rev Immunol 2007; 25:21-50; PMID:17029568; http://dx.doi.org/10.1146/annurev.immunol.25.022106.141702
15. Jefferis R. Isotype and glycoform selection for antibody therapeutics. Arch Biochem Biophys 2012; 526:159-66; PMID:22465822; http://dx.doi.org/10.1016/j.abb.2012.03.021
16. Shi HH, Goudar CT. Recent advances in the understanding of biological implications and modulation methodologies of monoclonal antibody N-linked high mannose glycans. Biotechnol Bioeng. 2014 Oct;111(10):1907-19; PMID:24975601; http://dx.dpoi.org/10.1002/bit.25318.
17. Meibohm B. Protein engineering for improved pharmacologic characteristics of established monoclonal antibody-based therapeutics. Clin Pharmacokinet 2014; 53:863-4; PMID:25212704; http://dx.doi.org/10.1007/s40262-014-0186-6
18. Goetze AM, Liu YD, Zhang Z, Shah B, Lee E, Bondarenko PV, Flynn GC. High-mannose glycans on the Fc region of therapeutic IgG antibodies increase serum clearance in humans. Glycobiology 2011; 21:949-59; PMID:21421994; http://dx.doi.org/10.1093/glycob/cwr027
19. Kanda Y, Yamada T, Mori K, Okazaki A, Kitajima-Miyama K, Kuni-Kamochi R, Nakano R, Yano K, Shitara K, Satoh M. Comparison of biological activity among nonfucosylated therapeutic IgG1 antibodies with three different N-linked Fc oligosaccharides: the high-mannose, hybrid, and complex types. Glycobiology 2007; 17:104-18; PMID:17012310; http://dx.doi.org/10.1093/glycob/cwl057
20. Othman O, Tran JQ, Tang MT, Dutta S. Population pharmacokinetics of daclizumab high-yield process in healthy volunteers: integrated analysis of intravenous and subcutaneous, single- and multiple-dose administration. Clin Pharmacokinet 2014; 53:907-18; PMID:25212703; http://dx.doi.org/10.1007/s40262-014-0159-9
21. Wiendl H, Gross CC. Modulation of IL-2Rα with daclizumab for treatment of multiple sclerosis. Nat Rev Neurol 2013; 9:394-404; PMID:23732529; http://dx.doi.org/10.1038/nrneurol.2013.95
22. Huss DJ, Mehta DS, Sharma A, You X, Riester KA, Sheridan JP, Amaravadi LS, Elkins JS, Fontenot JD. In vivo maintenance of human regulatory T cells during CD25 blockade. J Immunol 2015; 194:84-92; PMID:25416807; http://dx.doi.org/10.4049/jimmunol.1402140
23. Fontenot JD, Rasmussen JP, Gavin MA, Rudensky AY. A function for interleukin 2 in Foxp3-expressing regulatory T cells. Nat Immunol 2005; 6:1142-51; PMID:16227984; http://dx.doi.org/10.1038/ni1263
24. Sakaguchi S, Yamaguchi T, Nomura T, Ono M. Regulatory T cells and immune tolerance. Cell 2008; 133:775-87; PMID:18510923; http://dx.doi.org/10.1016/j.cell.2008.05.009
25. Josefowicz SZ, Lu LF, Rudensky AY. Regulatory T cells: mechanisms of differentiation and function. Annu Rev Immunol 2012; 30:531-64; PMID:22224781; http://dx.doi.org/10.1146/annurev.immunol.25.022106.141623
26. Amado IF, Berges J, Luther RJ, Mailhé MP, Garcia S, Bandeira A, Weaver C, Liston A, Freitas AA. IL-2 coordinates IL-2-producing and regulatory T cell interplay. J Exp Med 2013; 210:2707-20; PMID:24249704; http://dx.doi.org/10.1084/jem.20122759
27. Giovannoni G, Radue EW, Havrdova E, Riester K, Greenberg S, Mehta L, Elkins J. Effect of daclizumab high-yield process in patients with highly active relapsing-remitting multiple sclerosis. J Neurol 2014; 261:316-23; PMID:24375015; http://dx.doi.org/10.1007/s00415-013-7196-4
28. Hori T, Uchiyama T, Tsudo M, Umadome H, Ohno H, Fukuhara S, Kita K, Uchino H. Establishment of an interleukin 2-dependent human T cell line from a patient with T cell chronic lymphocytic leukemia who is not infected with human T cell leukemia/lymphoma virus. Blood 1987; 70:1069-72; PMID:3115332